

Entangled mixed-state generation by twin-photon scattering

G. Puentes¹, D. Voigt^{1,2}, A. Aiello¹, and J.P. Woerdman¹

¹*Huygens Laboratory, Leiden University, P.O. Box 9504, 2300 RA Leiden, The Netherlands.*

²*Cosine Research bv, Niels Bohrweg 11, 2333 CA Leiden, The Netherlands.*

We report novel experimental results on mixed-state generation by multi-mode scattering of polarization-entangled photons. By using a large variety of scattering media we obtain two markedly different classes of scattered states; namely Werner-like and sub-Werner-like states. Our experimental findings are in excellent agreement with a phenomenological model based upon the description of a scattering process as a quantum map.

PACS numbers: 03.67.Mn, 42.50.Ct, 42.50.Dv, 42.65.Lm

The study of spatial, temporal, and polarization correlations of light scattered by inhomogeneous and turbid media has a history of more than a century [1]. Due to the high complexity of scattering media only single-scattering properties are known at a microscopic level [2], whereas for multiple-scattering the emphasis is on macroscopic theoretical descriptions of the correlation phenomena [3]. In most examples of the latter [4, 5, 6, 7] the intensity correlations of the interference pattern generated by multiple scattered light are explained in terms of *classical* wave coherence. On the other hand, the recent availability of single-photon sources has triggered the interest in *quantum* correlations of multiple scattered light [8]. Generally speaking, the quantum correlations of the scattered photons will depend on the quantum state of the light illuminating the sample. In Ref. [8], spatial quantum correlations of scattered light were analyzed for Fock, coherent and thermal input states.

In this Letter we present the first experimental results on quantum polarization correlations of scattered photons pairs. Specifically, we study the entanglement content in relation to the polarization purity of multiple-scattered twin-photons, initially generated in a polarization-entangled state by spontaneous parametric down-conversion (SPDC). The initial entanglement of the input photon pairs will in general be degraded by multiple scattering. This can be understood by noting that the scattering process distributes the initial correlations of the twin-photons over the many spatial modes excited along the propagation in the medium. In the case of spatially inhomogeneous media the polarization degrees of freedom are coupled to the spatial degrees of freedom generating polarization dependent speckle patterns. If the spatial correlations of such patterns are averaged out by multi-mode detection, the polarization state of the scattered photon(s) is reduced to a mixture, and the resulting polarization-entanglement of the photon pairs is degraded with respect to the initial one. This theoretical background has been elaborated in [9, 10].

The experimental set-up is shown in Fig.1. A krypton-ion laser at 413.1 nm pumps a 1-mm thick BBO crystal, where polarization-entangled photons are created by

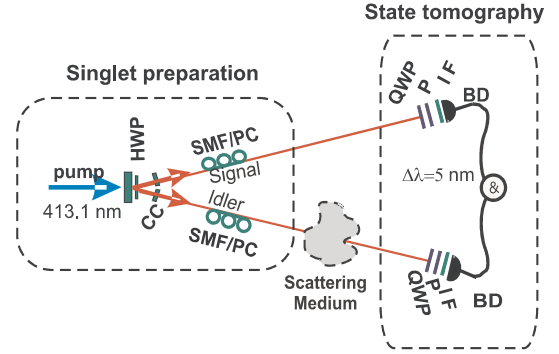


FIG. 1: (Color online) Experimental scheme: After singlet preparation, the idler photon propagates through the scattering medium. The polarization state of the scattered photon-pairs is then reconstructed via a quantum tomographic procedure (see text for details).

SPDC in a degenerate type II phase-matching configuration at 826.2 nm. Single-mode fibers (SMF) are used as spatial filters to assure that the initial state is in a single transverse mode. Polarization controllers (PC) align the axes of the spurious birefringence along the SMFs in the SPDC crystal basis. The total retardation introduced by the SMFs and walk-off effects at the BBO crystal are compensated by additional BBO crystals (0.5 mm thick) in both signal and idler paths, together with a half-wave plate (HWP) [11]. The polarization analyzer used for quantum tomography consists of a quarter-wave plate (QWP) followed by a polarizer (P) in both arms. Additionally, $\Delta\lambda = 5$ nm interference filters (IF) are used for bandwidth selection. Finally, the photon pairs are detected in a multi-transverse mode fashion by using momentum-insensitive or “bucket” detectors (BD). The photon pairs incident on the scattering medium are initially prepared in the maximally entangled singlet Bell state $|\psi^-\rangle = (|HV\rangle - |VH\rangle)/\sqrt{2}$, where H and V are labels for horizontal and vertical polarizations of the two photons, respectively. Our experimental singlet state has a fidelity [12] of 98% with the theoretical target state.

All the scattering media that we analyzed were *local*, i.e., they were located in the path of *one* photon of the

entangled-pair (the idler one). The three general categories of media we used were: (type I) isotropic scattering media, the scattering properties of which are polarization independent; (type II) birefringent scattering media, these are anisotropic scatterers which introduce a polarization dependent retardation; and (type III) dichroic scattering media, which are anisotropic scatterers with polarization dependent losses. A detailed description of the depolarizing properties of the several scatterers used is given in [13].

The degree of entanglement and mixedness of the photon pairs were quantified by the tangle (T), i.e., the concurrence squared [14], and the linear entropy [S_L] [15]. These quantities were calculated from the 4×4 polarization density matrix ρ of the scattered photons, by using $T(\rho) = (\max\{0, \lambda_1 - \lambda_2 - \lambda_3 - \lambda_4\})^2$, where $\lambda_1^2 \geq \lambda_2^2 \geq \lambda_3^2 \geq \lambda_4^2$ are the eigenvalues of $\rho(\sigma_2 \otimes \sigma_2)\rho^*(\sigma_2 \otimes \sigma_2)$, with σ_2 a Pauli matrix [14], and $S_L(\rho) = \frac{4}{3}[1 - \text{Tr}(\rho^2)]$ [15]. The density matrix ρ was in turn reconstructed via maximum likelihood tomography [16]. Fig.2 (a) and

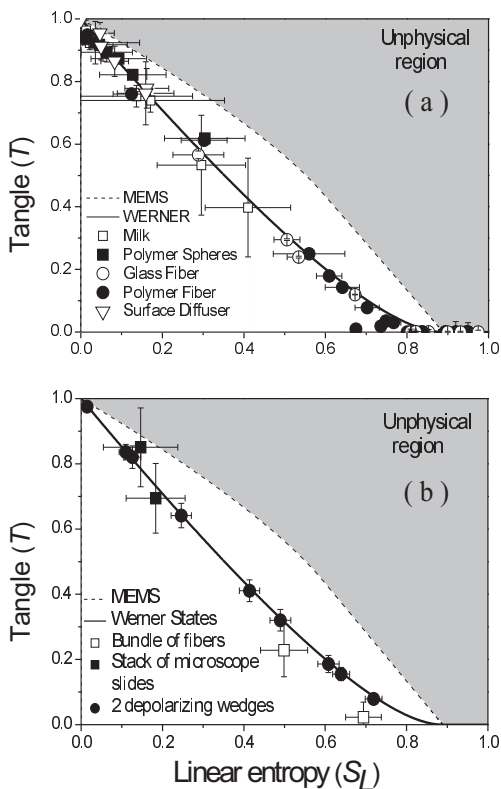


FIG. 2: Experimental data in the tangle (T)-linear entropy (S_L) plane. The grey area corresponds to unphysical density matrices. Dashed curve: Maximally entangled mixed states (MEMS), solid curve: Werner states. Fig. 2 (a) Isotropic scatterers (type I): glass and polymer multi-mode fibers, milk and microspheres diluted in water, surface diffusers; Fig. 2 (b) Birefringent scatterers (type II): two depolarizing wedges in cascade, bundle of fibers, stacks of microscope slides.

(b) show typical tangle vs. linear entropy diagrams. The grey area corresponds to non-physical states [17]. The dashed curve which bounds the physical region is given by the maximally entangled mixed states (MEMS) [18], while the solid curve corresponds to Werner states $\rho_W = r|\psi^-\rangle\langle\psi^-| + \frac{(1-r)}{4}I$, ($0 \leq r \leq 1$) [19]. Fig.2 (a) shows experimental data corresponding to isotropic scatterers (type I). Specifically: suspensions of milk and micro-spheres, where the sample dilution was varied to obtain different points; multi-mode glass and polymer fibers where the tuning parameter was the length of the fiber (cut-back method); and surface diffusers, where the full width scattering angle was used as tuning knob. Note that suspensions of milk and micro-spheres are *dynamic* media, where Brownian motion of the micro-particles induces temporal fluctuations within the detection integration time. Each point in Fig.2 (a-b) corresponds to a tomographically reconstructed density matrix. At the top-left corner ($T = 1, S_L = 0$) we find the data corresponding to the initial singlet state. As the scattering sample becomes thicker the data shifts toward the bottom-right corner ($T = 0, S_L = 1$), which corresponds to a fully mixed state.

Fig.2 (b) displays experimental data for birefringent scattering media (type II). We analyzed two categories of type b media: the first one consisted of two wedge depolarizers in cascade [20], where the different points are obtained for different relative angles between the principal axes of the two wedges [21]. The second one consisted of samples with “topological” birefringence due to their special symmetry properties. Within this latter category we studied two systems. The first was a bundle of parallel fibers [22], where the scattering takes place roughly in a plane. The second system was a stack of parallel microscope slides (with uncontrolled air layers in between), which provide depolarization due to the wave-vector spread of the input beam that enters, via a SMF (NA=0.12), from the side of the stack and travels in the plane of the slides. Fig.2 reveals that all the data, corresponding to samples of types a and b, fall on the Werner curve, within the experimental error.

Close inspection of the reconstructed density matrices for these scattering media revealed that in some cases the measured states represent a generalized form of Werner states, which we call Werner-like states. These are equivalent to the original ρ_W with respect to their values of T and S_L , but their density matrices are not isotropic. In fact, Werner states ρ_W of bipartite systems were originally defined [19] as such states which are $U \otimes U$ invariant: $\rho_W = U \otimes U \rho_W U^\dagger \otimes U^\dagger$. Here $U \otimes U$ is any symmetric separable unitary transformation acting on the two subsystems. The generalized Werner states ρ_{GW} are obtained from ρ_W by applying an arbitrary unitary operation V upon only one of the two subsystems: $\rho_{GW} = V \otimes I \rho_W V^\dagger \otimes I$. In this way, the generalized Werner states are equivalent to the original ρ_W with respect to T and

S_L (since a local unitary transformation can not affect the degree of entanglement or the degree of purity) but are no longer invariant under unitary transformations of the form $U \otimes U$. By parameterizing $V = V(\alpha, \beta, \gamma)$, with α, β, γ the three Euler angles, we calculated the average maximal fidelity of the measured states ρ_m with the target generalized Werner states $\rho_{GW}(r, \alpha, \beta, \gamma)$. We found $f(\rho_m, \rho_{GW}) = 0.969 \pm 0.003$, revealing that our data is well fitted by this four-parameter class of Werner states. In Fig. 3, we show the data obtained for dichroic scat-

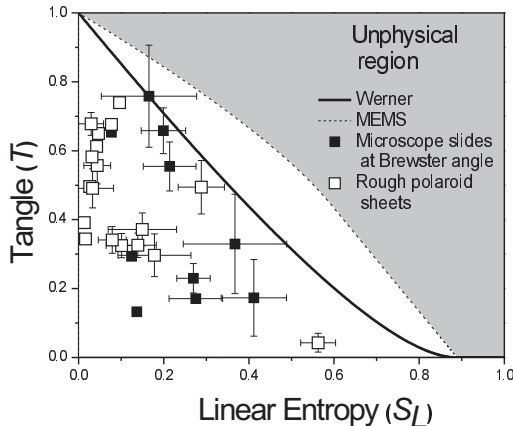


FIG. 3: Experimental data corresponding to dichroic scattering samples (type III): Stacks of microscope slides at Brewster angle with surface diffusers and rough polaroid sheets.

tering systems (type III). These consisted of two kinds; namely (i) a surface diffuser followed by a stack of microscope slides at the Brewster angle, and (ii) a commercially available polaroid sheet with manually-added surface roughness on its front surface to provide the scattering. All the data obtained for dichroic scattering media fall below the Werner curve, generating thus sub-Werner like states; namely states with a lower value of T than a Werner state, for a given value of S_L . The markedly different behavior, with respect to samples type I and type II, comes from the fact that samples type III do not just add a local unitary operation to one of the two photons, as they introduce polarization dependent losses to the problem.

Now, we compare the measured data with a phenomenological model that relates the classical Mueller matrix M representing the scattering medium with the twin-photon polarization density matrix ρ [23]. Any physical scattering process that transforms the generic input two-photon state ρ_{in} into the output two-photon state ρ_{out} , can be described in terms of a linear, completely positive map \mathcal{E} such that:

$$\rho_{\text{out}} = \mathcal{E}[\rho_{\text{in}}] = \sum_{\mu=0}^3 K_{\mu} \rho_{\text{in}} K_{\mu}^{\dagger}, \quad (1)$$

where $\sum_{\mu} K_{\mu}^{\dagger} K_{\mu} = I$ for trace-preserving maps [24]. We

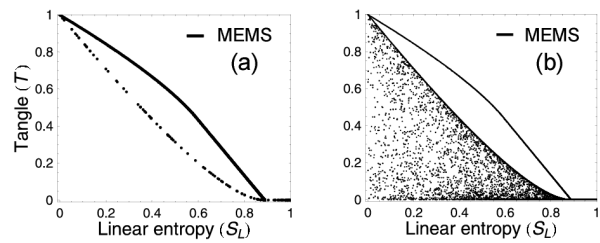


FIG. 4: Numerical simulation for our phenomenological model. (a) Isotropic and birefringent scattering, (b) dichroic scattering. Solid upper-curve corresponds to MEMS states.

anticipate here that such condition cannot be fulfilled by maps describing *dichroic* scatterers (we shall discuss this issue below). In our experiment the scattering medium acts on a single photon, this implies that each operator K_{μ} can be factorized as $K_{\mu} = J_{\mu} \otimes I$, where each J_{μ} can be thought as a *classical* 2×2 Jones matrix representing some polarization properties of the scattering medium. Thus, a relation between the quantum map \mathcal{E} and the classical Jones matrices $\{J_{\mu}\}$ can be established [23]. In particular, it is possible to show that the Mueller matrix M describing the classical polarization properties of the scattering medium can be written in terms of the elements J_{μ} of the quantum map \mathcal{E} as:

$$M = \Lambda^{\dagger} \left(\sum_{\mu=0}^3 J_{\mu} \otimes J_{\mu}^* \right) \Lambda, \quad (2)$$

where an explicit expression for the unitary matrix Λ can be found in Ref. [23]. Equation (2) can be inverted in order to find the set of four Jones matrices $\{J_{\mu}\}$ generating M . In this way, if we know the classical Mueller matrix M describing a given scattering medium, we can write down immediately the corresponding quantum map \mathcal{E} by inverting Eq. (2). With these ingredients, a phenomenological polarization-scattering model can be built. First we write an arbitrary Mueller matrix M as the product $M = M_{\Delta} M_B M_D$, where M_{Δ} , M_B and M_D represent a purely depolarizing element, a birefringent (or retarder) element, and a dichroic (or diattenuator) element, respectively [25]. Second, we invert Eq. (2) to find the quantum maps corresponding to M_{Δ} , M_B , and M_D and, by using such maps, we calculate the scattered two-photon state ρ_{out} . In our experimental set-up we have isotropic scatterers M_{Δ} with isotropic depolarization factor $0 \leq \Delta < 1$, birefringent scattering media which can be described in terms of the product of an isotropic depolarizer and a purely birefringent medium by $M_B M_{\Delta}$, and dichroic media which are described as a product of an isotropic depolarizer and a purely dichroic medium by $M_D M_{\Delta}$. Analytical expressions for general M_{Δ} , M_B and M_D are given in the literature [20]. Using random numbers selected from suitably chosen ranges

for the independent elements of these matrices, we simulated the scattering processes occurring in our set-ups. Fig. 4 shows a numerical simulation of scattered states in the tangle vs. linear entropy plane, obtained with the singlet two-photon state as input state. Fig. 4 (a) refers to isotropic and birefringent scatterers, and Fig. 4 (b) to dichroic scatterers. The qualitative agreement between these model calculations and the experimental results shown in Fig. 2 and Fig. 3 is manifest.

In the case of sub-Werner states, the phenomenological model represents a non-trace preserving map. Such description might be considered controversial since a non-trace preserving local map can, in principle, lead to violation of causality when it describes the evolution of a composite system made of two spatially separate subsystems [26]. However, we argue that our measured states do not violate the no-signalling condition as they are post-selected by the coincidence measurement, a procedure that involves causal classical communication between the two detectors.

In conclusion, we have presented experimental results on entanglement properties of scattered photon-pairs for three varieties of local scattering media. In this way we were able to generate two distinct types of mixed states; namely Werner-like and sub-Werner-like states. The former correspond to a generalized class of Werner states. Our experimental results are in excellent agreement with our phenomenological model. Finally, we expect it to be possible to create states *above* the Werner curve [17] (in particular MEMS), by post-selective detection when acting on a single photon [26]. Work along this line is in progress in our group.

This project is part of the program of FOM and is also supported by the EU under the IST-ATESIT contract.

We gratefully acknowledge M. B. van der Mark for making available the bundle of parallel fibers [22].

-
- [1] Lord Rayleigh, *Philos. Mag.* **47**, 375 (1899); *Proc. Roy. Soc. London, Ser. A* **79**, 399 (1907).
 [2] H. C. van de Hulst, *Light Scattering by Small Particles* (Dover, New York, 1981).

- [3] M. C. W. van Rossum and Th. M. Nieuwenhuizen, *Rev. Mod. Phys.* **71**, 313 (1999).
 [4] M. P. Van Albada, and A. Lagendijk, *Phys. Rev. Lett.* **55**, 2692 (1985).
 [5] A. A. Chabanov, M. Stoytchev, and A. Z. Genack, *Nature (London)* **404**, 850 (2000).
 [6] G. L. J. A. Rikken and B. A. van Tiggelen, *Nature (London)* **381**, 54 (1996).
 [7] I. Freund, M. Rosenbluh, and S. Feng, *Phys. Rev. Lett.* **61**, 2328 (1988).
 [8] P. Lodahl, A. P. Mosk, and A. Lagendijk, *Phys. Rev. Lett* **95**, 173901 (2005).
 [9] A. Aiello and J. P. Woerdman, *Phys. Rev. A* **70**, 023808 (2004).
 [10] J. L. van Velsen and C. W. J. Beenakker, *Phys. Rev. A* **70**, 032325 (2004).
 [11] P. G. Kwiat, K. Mattle, H. Weinfurter, A. Zeilinger, A. V. Sergienko, and Y. Shih, *Phys. Rev. Lett.* **75**, 4337 (1995).
 [12] R. Jozsa, *J. Mod. Opt.* **41**, 2315 (1994).
 [13] G. Puentes, D. Voigt, A. Aiello, and J. P. Woerdman, *Opt. Lett.* **30**, 3216 (2005).
 [14] W. K. Wootters, *Phys. Rev. Lett.* **80**, 2245 (1998).
 [15] S. Bose, and V. Vedral, *Phys. Rev. A* **61**, 040101(R) (2000).
 [16] D. F. V. James, P. G. Kwiat, W. J. Munro, and A. G. White, *Phys. Rev. A* **64**, 052312 (2001).
 [17] N. A. Peters, J. B. Altepeter, D. A. Branning, E. R. Jeffrey, T. C. Wei, and P. G. Kwiat, *Phys. Rev. Lett.* **92**, 133601 (2004).
 [18] W. J. Munro, D. F. V. James, A. G. White, and P. G. Kwiat, *Phys. Rev. A* **64**, 030302(R) (2001).
 [19] R. F. Werner, *Phys. Rev. A* **40**, 4277 (1989).
 [20] D. S. Kliger, J. W. Lewis, and C. E. Randall, *Polarized Light in Optics and Spectroscopy* (Academic Press, Inc., 1990).
 [21] G. Puentes, D. Voigt, A. Aiello, and J. P. Woerdman, to appear in: *Opt. Lett.* **31**, No. 13 (2006).
 [22] M. B. van der Mark, PhD thesis, Univ. Amsterdam (1990).
 [23] A. Aiello, and J. P. Woerdman, e-print math-ph/0412061.
 [24] M. A. Nielsen and I. L. Chuang, *Quantum Computation and Quantum Information* (Cambridge U. Press, 2000), Chap. 12.
 [25] S. Y. Lu and R. A. Chipman, *J. Opt. Soc. A* **13**, 1106 (1996).
 [26] A. Aiello, G. Puentes, D. Voigt, and J. P. Woerdman, e-print quant-ph/0603182.